Materials Today Bio 26 (2024) 101070

Contents lists available at ScienceDirect

Materials Today Bio

journal homepage: www.journals.elsevier.com/materials-today-bio

Amplifying endogenous stem cell migration for *in situ* bone tissue formation: Substance P analog and BMP mimetic peptide-loaded click-crosslinked hyaluronic acid hydrogel

Hee Eun Kim [a,1], Hyeon Jin Ju [a,1], Shina Kim [a,1], Young Hun Kim [a], Soyeon Lee [a], Sangdun Choi [a], Hyun C. Yoon [a], Hak Soo Choi [b,**], Moon Suk Kim [a,c,*]

[a] Department of Molecular Science and Technology, Ajou University, Suwon, 16499, South Korea
[b] Gordon Center for Medical Imaging, Department of Radiology, Massachusetts General Hospital and Harvard Medical School, Boston, MA, 02114, USA
[c] Research Institute, Medipolymer, Woncheon Dong 274, Suwon, 16522, South Korea

ARTICLE INFO

Keywords:
Endogenous stem cell
Substance P analog peptide
BMP-2 mimetic peptide
In situ osteogenic differentiation
Hyaluronic acid
Scaffold

ABSTRACT

Endogenous stem cell-driven *in situ* bone tissue formation has recently garnered increasing attention. Therefore, our study sought to refine methods to enhance the migration and subsequent osteogenic differentiation of these cells. Our innovative approach involves using an injectable hydrogel that combines click cross-linking sites and a BMP-2 mimetic peptide (BP) with hyaluronic acid (HA). This injectable formulation, hereinafter referred to as SPa + Cx-HA-BP, incorporates a substance P analog peptide (SPa) with Cx-HA-BP, proving versatile for *in vitro* and *in vivo* applications without cytotoxicity. The controlled release of SPa creates a gradient that guides endogenous stem cells towards the Cx-HA scaffold from specific tissue niches. Both Cx-HA and SPa+Cx-HA induced minimal changes in the expression of genes associated with osteogenic differentiation. In contrast, these genes were robustly induced by both SPa + Cx-HA+BP and SPa + Cx-HA-BP, in which BP was respectively integrated via physical and chemical methods. Remarkably, chemically incorporating BP (Cx-HA-BP) resulted in 4–9 times higher osteogenic gene expression than physically mixed BP in Cx-HA+BP. This study validates the role of SPa role in guiding endogenous stem cells toward the hydrogel and underscores the substantial impact of sustained BP presence within the hydrogel. Collectively, our findings offer valuable insights for the development of innovative strategies to promote endogenous stem cell-based tissue regeneration. The developed hydrogel effectively guides stem cells from their natural locations and facilitates sustained osteogenic differentiation, thus holding great promise for applications in regenerative medicine.

1. Introduction

Regenerative medicine, which integrates stem cells and biologically active molecules for therapeutic purposes, is at the forefront of innovative approaches for rejuvenating damaged tissues and organs [1]. In this field, biomedical strategies often entail the use of stem cells or progenitor cells, either alone or in combination with biologically active molecules within a scaffold. These constructs are subsequently transplanted into the human body, which has recently become the subject of extensive research [2]. Notably, advancements in regenerative medicine have increasingly focused on the utilization of endogenous cells present in tissues or organs for self-regeneration [3–5]. In this context, chemoattractants such as substance P (SP) have emerged as effective tools for activating and mobilizing endogenous stem cells from specific tissue niches toward specific scaffolds [6–8].

In one of our recent studies in which we examined the binding force between SP and the neurokinin 1 receptor (NK1R), we discovered an SP analog peptide (SPa) that efficiently induces the migration of endogenous stem cells [9]. Studies have demonstrated that SPa-loaded scaffolds enhance the migration of human mesenchymal stem cells (hMSCs) by approximately 2.5-fold compared to an SP-loaded scaffold. Building on these findings, our study sought to explore the potential of endogenous

* Corresponding author.
** Corresponding author.
E-mail addresses: hchoi12@mgh.harvard.edu (H.S. Choi), moonskim@ajou.ac.kr (M.S. Kim).
[1] These authors contributed equally to this work.

https://doi.org/10.1016/j.mtbio.2024.101070
Received 30 January 2024; Received in revised form 20 April 2024; Accepted 25 April 2024
Available online 27 April 2024

stem cells to migrate to the scaffold and undergo differentiation into specific tissues, thereby facilitating *in situ* tissue regeneration without the direct injection of hMSCs. Furthermore, the bone morphogenetic protein (BMP) mimetic peptide (BP) was used as a cost-effective and stable alternative to BMP for bone tissue regeneration [10–12]. To ensure the efficient incorporation of peptides, injectable hydrogels are widely used in tissue engineering because they remain in a liquid state prior to injection and solidify once they are injected [13–15]. Hyaluronic acid (HA) is among the most widely used natural biomaterials in biomedical applications [16–18]. Moreover, BP can be incorporated into the hydrogel scaffold to enhance its *in vivo* properties. This is achieved through a biorthogonal Diels–Alder click crosslinking reaction between tetrazine (TE) and transcyclooctene (TC) to create a click crosslinked-hyaluronic acid (Cx-HA) hydrogel scaffold. This scaffold, formed by mixing TE-HA and TC-HA, exhibits prolonged residence times under physiological conditions [19–21].

In this study, we designed SPa + Cx-HA-BP hydrogels by chemically incorporating BP into Cx-HA and physically integrating SPa into the hydrogel to facilitate the migration of endogenous stem cells by releasing SPa. This SPa + Cx-HA-BP scaffold exhibits promising potential for endogenous stem cell-based *in situ* osteogenic differentiation. The two primary objectives of this study were to (1) assess the efficacy of endogenous stem cell migration induced by SPa release from Cx-HA-BP and (2) evaluate whether the Cx-HA-BP scaffold promotes *in situ* osteogenic differentiation through the migration of endogenous stem cells from their original tissues. This pioneering research holds the potential to revolutionize bone tissue regeneration by activating endogenous stem cells, providing a glimpse into the future of regenerative medicine.

2. Experimental section

2.1. Materials

Hyaluronic acid (HA) (1 MDa, Humedix, Anyang, Korea), methyltetrazine-PEG4-amine hydrochloride salt (Click Chemistry Tools, AZ, USA), *trans*-cyclooctene-amine hydrochloride salt (Click Chemistry Tools, AZ, USA) and 4-(4,6-dimethoxy-1,3,5-triazin-2-yl)-4-methylmorpholinium chloride (DMTMM) (Tokyo chemical industry, Tokyo, Japan) and Substance P (SP; RPKPQQFFGLM) (GenScript, NJ, USA) were used as received. Substance P analog (SPa; RISPQQRDALA), BMP-2 mimetic peptide (BP; KIPKASSVPTELSAISTLYL), fluorescein isothiocyanate-conjugated SPa (SPa-F), fluorescein isothiocyanate-conjugated SP (SP–F), fluorescein isothiocyanate-conjugated BP (BP–F) were purchased from Biostem (Suwon, Korea). 1,4-[D]iaminobutane (Sigma, MO, USA), protamine, sodium azide, propargyl amine, IR-783, indocyanine green (ICG) and PKH26 red fluorescent cell linker kit were purchased from Sigma (MO, USA). Low-glucose Dulbecco's modified Eagle's medium (DMEM), Dulbecco's phosphate-buffered saline (DPBS), penicillin-streptomycin (PS), 0.05 % trypsin-EDTA and fetal bovine serum (FBS) were purchased from Gibco BRL (Carlsbad, CA, USA).

2.2. hMSCs culture and labeling of hMSCs

hMSCs (passage 2) purchased from LONZA (Basel, Switzerland) were cultured as described in the Supporting Information, and hMSCs from passage 6 were used in this experiment. hMSCs at passage 6 were labeled with PKH26 (PKH-hMSCs) and ICG (ICG-hMSCs) as described in the Supporting Information.

2.3. In vitro osteogenic differentiation of hMSCs in the presence of BMP-2 or BP

hMSCs were cultured in a 24-well plate at 1×10^4 cells per well. After 24 h, control group was treated with osteogenic differentiation media (DMEM + 5 % FBS + 1 % PS + 10 nM dexamethasone + 50 μM L-ascorbic acid-2-phosphate + 10 mM b-glycerophosphate + 2 mM L-glutamine). The group treated by BMP-2 or BP was cultured using BMP-2 media (Osteogenic differentiation media +50 ng/mL BMP-2) or BP media (Osteogenic differentiation media +100 μM BP). All group was cultured for 4 weeks. The medium was replaced once every 3 days. To proceed with Von Kossa (VK) staining, hMSCs treated by BMP-2 or BP (including control) were washed twice with PBS and fixed with 4 % paraformaldehyde for 30 min. The fixed cells were washed twice with PBS, treated with 5 % silver nitrate solution (Sigma, MO, USA) and irradiated with UV light at room temperature for 60 min. Then it was washed twice with deionized water (DW), treated with 5 % sodium thiosulfate (StatLab, TX, USA) at room temperature for 2 min, and washed twice with DW. Then Nuclear Fast Red (Cepham Life Science, MD, USA) was treated at room temperature for 5 min and washed with DW. To proceed with Alizarin Red S (ARS) staining, hMSCs treated by BMP-2 or BP (including control) were washed twice with PBS and fixed with 4 % paraformaldehyde for 30 min. The fixed cells were washed twice with PBS, treated with 500 μL of 0.2 % ARS solution at room temperature for 15 min and washed with DW. All experiments were performed at least three times. The stained cells were observed using LSM 710 laser scanning microscope (Carl Zeiss Microscopy GmbH, Jena, Germany) and AxioVision Sotftware (Carl Zeiss Microscopy GmbH, Jena, Germany).

The osteogenic differentiation of hMSCs was examined by the RT-PCR. At 1, 2, 3 and 4 weeks, mRNA from hMSCs treated by BMP-2 or BP (including control) was extracted by TRIzol (Invitrogen, CA, USA). The concentration was measured at 260 nm using ND-1000 spectrophotometer (NanoDrop Technologies, DE, USA). 50 ng of extracted RNA was reverse transcribed using the SuperScript III First-Strand Kit (Invitrogen, CA, USA) to make cDNA. Then gene expression was confirmed by performing real-time PCR using AriaMx Real-Time PCR System (Agilent, CA, USA) and Power SYBR Green (Applied Biosystems, MA, USA). The gene of glyceraldehyde 3-phosphate dehydrogenase (GAPDH) was used as a reference. Gene expression was compared using the comparative threshold cycle (Ct) method ($2^{-\Delta\Delta Ct}$). Detailed information on the primers (GenoTech, Daejeon, Korea) used in the *in vitro* osteogenic differentiation experiments of hMSCs is provided in the Supporting Information (Table S1).

2.4. Preparation of injectable formulation of Cx-HA

To prepare the Cx-HA, firstly the TE-HA and TC-HA were prepared according to previous work as described in the Supporting Information [19]. Then, the prepared TE-HA and TC-HA were each dispersed in PBS (pH 7.4) to a final concentration of 20 mg/mL. The TE-HA and TC-HA solutions were loaded separately into each compartment of a dual-barrel syringe (donated by Ewha Biomedics, Seoul, Korea). Cx-HA was prepared by simultaneous injection from each part of the dual-barrel syringe into a vial for subsequent characterization.

2.5. Preparation of BP-labeled TE-HA, BP-labeled TC-HA, and Cx-HA-BP

TE-HA (10 mg/mL) and TC-HA (10 mg/mL) were solubilized and reacted with DMTMM (0.3 mg, 0.001 mmol) at room temperature for 1 h to activate carboxyl group of TE-HA and TC-HA. Then BP (21 mg, 0.01 mmol) was added into each activated TE-HA and TC-HA solution and stirred at room temperature for 24 h. Unreacted BP was removed via dialysis over 3 days with a molecular weight cutoff (MWCO) dialysis tube of 3.5–5 kDa. Then the dialyzed solution was freeze-dried using a freeze dryer (MLB-9003, Mareuda, Gwangju, Korea) to obtain pure TE-HA-BP and TC-HA-BP (Chemically BP bound to TE-HA and TC-HA). Finally, elemental analysis of TE-HA-BP (C: 43.9 %, H: 6.4 %, N: 5.4 %) and TC-HA-BP (C: 41.4 %, H: 5.8 %, N: 3.8) was obtained (Table S2). The BP physically mixed with TE-HA and TC-HA was abbreviated as TE-HA + BP and TC-HA+BP. The SP or SPa physically mixed with TE-HA

and TC-HA was abbreviated as SP (or SPa) + TE-HA and SP (or SPa) + TC-HA. Each formulation [HA alone], [TE-HA+BP and TC-HA+BP], [TE-HA-BP and TC-HA-BP], [SP (or SPa) + TE-HA and SP (or SPa) + TC-HA], [(SPa + TE-HA+BP and SP + TC-HA+BP] and [SPa + TE-HA-BP and SPa + TC-HA-BP] were dispersed in PBS (pH 7.4) to a final concentration of 20 mg/mL. Each injectable formulation was loaded separately into each compartment of a dual-barrel syringe.

2.6. Rheological and SEM measurements

HA, Cx-HA, Cx-HA+BP and Cx-HA-BP were each dispersed in PBS (pH 7.4) to a final concentration of 20 mg/mL. The rheological properties of each solution were analyzed using an MCR 102 rheometer (Anton Paar, Austria) equipped with a politer temperature-controlled bottom plate and a parallel 25.0 mm stainless steel plate. All measurements were performed using Rheoplus/32 version V3.21 (Anton Paar) at 25 °C with a 0.3 mm gap at an oscillation frequency of 1 Hz with a fixed 2 % strain. All results of the experiment were expressed as the average results of three repeated measurements. For scanning electron microscopy (SEM) analysis, HA, Cx-HA, Cx-HA+BP and Cx-HA-BP were coated with a gold conductive layer using a plasma-sputtering apparatus (Emitech, K575, Kent, UK). SEM images were acquired using FE-SEM (JSM-6700F, JEOL, Tokyo, Japan).

2.7. Measurement of injection force

To examine the injection force of injectable formulation, the solution (100 μL) of [HA alone], [TE-HA and TC-HA], [TE-HA-BP and TC-HA-BP], [SPa + TE-HA and SPa + TC-HA] and [SPa + TE-HA-BP and SPa-TC-HA-BP], separately drawn into each barrel of a dual-barrel syringe with 26-gauge syringe (needle gauge: 26-G; 0.241 mm inner diameter and 13 mm in length). Injection force was determined using a WL2100 Instron Universal testing machine (WITHLAB, Gunpo, Korea) as described in the Supporting Information.

2.8. Preparation of near-infrared (NIR) fluorescence-labeled HA, TE-HA and TC-HA

IR-783-NH_2 was synthesized as outlined in the Supporting Information. For bioconjugation, HA, TE-HA, and TC-HA (10 mg/mL) were then solubilized in DW and reacted with DMTMM (16 mg, 0.057 mmol) at room temperature for 1 h to activate the carboxyl group of HA, TE-HA, and TC-HA. IR-783-NH_2 (30 mg, 0.038 mmol) was added into each activated HA, TE-HA, and TC-HA solution and stirred at room temperature for 24 h. Unreacted IR-783-NH_2 was removed via dialysis over 3 days with a molecular weight cutoff (MWCO) dialysis tube of 3.5–5 kDa. Then the dialyzed solution was freeze-dried using a freeze dryer to obtain pure HA-NIR, TE-HA-NIR, and TC-HA-NIR.

2.9. Evaluation of in vitro cytotoxicity of peptides (SPa or BP) or injectable hydrogel scaffolds

To evaluate the concentration-specific toxicity of SPa and BP on hMSCs, hMSCs were seeded in a 24-well plate at 1×10^4 cells per well, and after 24 h, SPa (0, 10, 50, 100, 200, 500 μg/mL) or BP (0, 0.5, 1, 2, 5, 10 mM) containing culture media was added into the well. Each media in the well was replaced every 3 days. Additionally, to evaluate the toxicity of Cx-HA, Cx-HA+BP, Cx-HA-BP, SPa + Cx-HA and SPa + Cx-HA-BP on hMSCs, hMSCs (1×10^4 cells per well) were seeded in bottom chamber of a 24 *trans*-well plate (SPL, Dajeon, Korea), and after 24 h, 100 μL of injectable formulation of [(TE-HA and TC-HA), (TE-HA(+BP) and TC-HA(+BP)), (TE-HA-BP and TC-HA-BP), (SPa + TE-HA and SPa + TC-HA) (total SPa amount of 100 μg/mL)) and (SPa + TE-HA-BP and SPa + TC-HA-BP) (total SPa amount of 100 μg/mL))] separately drawn into each barrel of a dual-barrel syringe were seeded in upper chamber (8.0 μm pore size) of a 24 *trans*-well plate. Each media in well was replaced every 3 days. To determine the cytotoxicity of peptides or injectable hydrogel scaffolds, media in the bottom chamber after the upper chamber was removed on days 1, 4, and 7 and washed once with DPBS. Then 500 μL of culture media and 50 μL of CCK-8 (Dojindo, MD, USA) were added in the bottom chamber. After incubation at 37 °C, 5.0 % CO_2 for 4 h, the absorbance at a wavelength of 450 nm was measured using a microplate reader (Molecular Devices, CA, USA). All results of the experiment were expressed as the average results of three repeated measurements.

2.10. In vitro migration of hMSCs

PKH-hMSCs that migrated into the 'wound field' were observed at 0, 12, and 24 h using Olympus IX51 inverted fluorescence microscope (Olympus, Tokyo, Japan) by Motic Images Advanced 3.2 software (Moitic Asia, Kowloon, Hong Kong). The amount of migrated hMSCs was determined on each image using ImageJ software (National Institutes of Health, Bethesda, MD, USA). All results of the experiment were expressed as the average results of three repeated measurements. The migration of hMSCs was evaluated by 'wound field' assay in order to evaluate the efficacy by SP or SPa and transwell migration assay in order to evaluate the efficacy by SP or SPa loaded Cx-HA hydrogel scaffold.

First, PKH-hMSCs (2×10^4 cells/well) suspended 70 μL of low serum media (DMEM + 2 % FBS + 1 % PS) were put into each insert of Culture-Insert 2 Well in μ-Dish 35 mm (IBIDI, Munich, Germany). hMSCs were incubated until they formed a monolayer on the insert for approximately 24 h. When the insert was removed, a 'wound field' was formed between the incubated hMSCs and then washed with PBS twice. 70 μL of low serum medium or SP (100 μg/mL) or SPa (100 μg/mL) solubilized low serum medium was individually added in the insert. Next, hMSCs migration by Cx-HA, SP + Cx-HA and SPa + Cx-HA was determined by transwell migration assay. The formulation (100 μL TE-HA and 100 μL TC-HA), (100 μL SP + TE-HA and SP + TC-HA) and (100 μL SPa + TE-HA and 100 μL SPa + TC-HA) separately drawn into each barrel of a dual-barrel syringe were seeded in bottom chamber of a 24 *trans*-well plate to form each hydrogel scaffold. PKH-hMSCs (2×10^4 cells per well) were seeded in upper chamber of a 24 *trans*-well plate. 500 μL of low serum media (DMEM + 2 % FBS + 1 % PS) was added in bottom chamber of a 24 *trans*-well plate and replaced once every 3 days. The amount of PKH-hMSCs migrated to the bottom chamber was observed by Olympus IX51 inverted fluorescence microscope at 1, 4, and 7 days by Motic Images Advanced 3.2 software. The amount of migrated hMSCs was determined on each image using ImageJ software. The amount of PKH-hMSCs as a control group without Cx-HA was also determined. Additionally, the amount of PKH-hMSCs migrated to the bottom chamber was determined by CCK-8 in the same way as described in the previous section. All results of the experiment were expressed as the average results of three repeated measurements.

2.11. In vitro osteogenic differentiation of hMSCs in Cx-HA, Cx-HA+BP, and Cx-HA-BP hydrogel scaffold

To evaluate the osteogenic differentiation of hMSCs on Cx-HA+BP and Cx-HA-BP, hMSCs (2 x 10^4 cells) were seeded on Cx-HA, Cx-HA+BP, and Cx-HA-BP-loaded 24-well plate and cultured with osteogenic differentiation media described in the previous section. The medium was replaced once every 3 days. At 1, 2, 3, and 4 weeks, osteogenic genes were evaluated by the same method described in the previous section 2.3.

2.12. Animal experiments

All experimental protocols involving live animals were approved by the Institutional Animal Care and Use Committee (Approval No. 2021-0084) of Ajou University School of Medicine. The *in vivo* experiments were conducted in accordance with guidelines approved by the Animal

Ethics Committee for Care and Use of Laboratory Animals of Ajou University Medical Center. All experiments were performed with BALB/c nude mice (20–22 g, 6 weeks) after anesthetizing them with 1:1:8 of Zoletil:Rumpun:Saline.

2.13. In vivo imaging of injectable formulations

The *in vivo* maintenance of the injectable formulations was compared by using HA-NIR and Cx-HA-NIR. HA-NIR was loaded into single-barrel syringes with 26 G needles. TE-HA-NIR and TC-HA-NIR were loaded into separate compartments of a dual-barrel syringe with a 26 G needle. Next, 200 μL HA-NIR or (100 μL TE-HA-NIR and 100 μL TC-HA-NIR) were injected subcutaneously into the dorsa of nude mice. The formulations contained the same concentration of NIR dye (20 mg/mL). NIR fluorescence images of the HA hydrogel scaffolds were obtained at a 730 nm excitation wavelength. The emitted light was filtered through a 750–825 nm bandpass filter with an exposure time of 500 ms and a gain of 1 using a dichroic MgF2 fused silica cube filter. Images were captured at specified time points using a FOBI fluorescence *in vivo* imaging system (NeoScience, Suwon, Korea).

2.14. In vivo migration of hMSCs toward the hydrogel scaffold

To observe hMSCs migration *in vivo* by SP or SPa released from hydrogel scaffold, 200 μL of Cx-HA or SPa + Cx-HA was injected subcutaneously into the mouse. ICG-labeling hMSCs was injected into the tail vein of a mouse. Control group was no injection of ICG-labeling hMSCs. NIR image appearing in the injected Cx-HA or SPa + Cx-HA and the control, was observed over time. NIR fluorescence images of the ICG-hMSCs were performed in the same method using a FOBI fluorescence *in vivo* imaging system with an exposure time of 2000 ms and a gain of 2 as described in the previous section.

2.15. In vivo release profiles of SPa-F from SPa-F-loaded hydrogel scaffolds

To evaluate *in vivo* release the SPa (or SP) from hydrogel scaffold, [200 μL SPa-F + HA, (100 μL SPa-F-TE-HA and 100 μL SPa-F-TC-HA) or (100 μL SP-F-TE- HA and 100 μL SP-F-TC-HA) and (100 μL SPa-F-TE-HA-BP and 100 μL SPa-F-TC-HA-BP) (total SPa-F or SP-F amount of 100 μg/mL) separately drawn into each barrel of a dual-barrel syringe] were injected subcutaneously into the dorsa of nude mice. Fluorescence intensity for FITC of SP-F was observed over time at a 460 nm excitation wavelength. The emitted light was filtered through a 515–555 nm bandpass filter with an exposure time of 500 ms and a gain of 1 using a dichroic MgF2 fused silica cube filter. Images were captured at specified time points using a FOBI fluorescence *in vivo* imaging system.

2.16. In vivo release profiles of BP-F from BP-F-loaded hydrogel scaffolds

To evaluate *in vivo* release the BP from hydrogel scaffold, [200 μL HA (+BP-F), (100 μL TE- HA(+BP-F) and 100 μL TC-HA(+BP-F)) and (100 μL TE-HA-BP-F and 100 μL TC-HA-BP-F) (total BP-F amount of 2 mM) separately drawn into each barrel of a dual-barrel syringe] were injected subcutaneously into the dorsa of nude mice. Fluorescence intensity for FITC of BP-F was observed using the same wavelength, filter, and exposure as that of SP-F, and the images were captured with the same FOBI fluorescence *in vivo* imaging system.

2.17. In vivo osteogenic differentiation of MSCs in the hydrogel scaffolds

To evaluate *in vivo* osteogenic differentiation of MSCs in the hydrogel scaffold, 100 μL of injectable formulation [(SPa-TE-HA and SPa-TC-HA) and (SPa-TE-HA-BP and SPa-TC-HA-BP) (total SPa amount of 100 μg/mL)) separately drawn into each barrel of a dual-barrel syringe] was injected subcutaneously into the dorsa of nude mice. Two experimental groups were divided into a group in which hMSCs were immediately injected into the tail vein of a mouse and a group in which no hMSCs were injected. After 2, 4, and 6 weeks, the hydrogel scaffold was removed from the mouse and fixed with 10 % formalin at room temperature for 7 days. The hydrogel scaffold was embedded with paraffin and sectioned to a thickness of 4 μm. Each section was incubated at 80 °C for 2 h and then immersed in xylene to remove excess paraffin. The sequential hydration was performed using 100 %, 95 %, 80 %, and 70 % ethyl alcohol and DW. The staining of Von Kossa (VK) and Alizarin Red S (ARS) of *in vivo* osteogenic differentiation at 2, 4, and 6 weeks was performed in the same method as described in the previous *in vitro* staining experiment. The stained cells were observed using LSM 710 laser scanning microscope and AxioVision software. The values of Von kossa and Alizarin red S positive staining (% Mineralized area) for each group using specialized imaging the ImageJ software (National Institutes of Health, MD, USA). The RT-PCRs of *in vivo* osteogenic differentiation at 2, 4 and 6 weeks were performed in the same method as described in the previous *in vitro* RT-PCR experiment. Detailed information on the primers (GenoTech, Daejeon, Korea) used in the *in vivo* osteogenic differentiation of mouse endogenous stem cells is provided in the Supporting Information (Table S1).

2.18. Statistical analysis

All the values of rheological, injectability properties, *in vitro* cytotoxicity, *in vitro* migration, and *in vitro* and *in vivo* gene expression were obtained from three independent experiments. All the data ($n = 3$) are presented as the mean and standard deviation (SD). To evaluate significance, the results were subjected to a one-way analysis of variance (ANOVA) with Bonferroni's multiple-comparison correction in the SPSS 12.0 software (IBM Corporation, NY, USA).

3. Results

3.1. In vitro osteogenic differentiation of hMSCs by BMP-2 or BP

As shown in Fig. 1, BP was chemically incorporated into TE-HA and TC-HA, whereas SPa was mixed with each hydrogel to form SPa + Cx-HA-BP for subcutaneous injection. Here, we designed a Cx-HA-BP scaffold for the sustained release of SPa, thereby stimulating the migration of endogenous stem cells for *in situ* osteogenic differentiation. Next, we assessed the *in vitro* osteogenic differentiation of hMSCs through the application of BMP-2 or BP. Following a 4-week incubation period, the osteogenically differentiated hMSCs were stained with Von Kossa and Alizarin Red S (Fig. 2a and b). Von Kossa revealed prominently black-stained images in the BMP-2 or BP-treated groups compared to the control group. During the incubation period, the black staining became progressively more intense, resulting in clearer and more numerous images in the BMP-2 or BP-treated groups. In Alizarin Red S staining, a distinct dark brown image emerged in the BMP-2 or BP-treated group, displaying progressively clearer stained areas compared to the control. Notably, the BMP-2-treated group exhibited slightly more differentiated images in both Von Kossa and Alizarin Red S staining compared to the BP-treated group.

To quantitatively assess the *in vitro* osteogenic differentiation of hMSCs induced by BMP-2 or BP, RT-PCR analyses were conducted to measure the gene expression levels of representative osteogenic markers, including RUNX2, ON, and OPN (Fig. 2c–e). The expression of RUNX2 and ON, both of which are representative markers of the early stages of osteogenic differentiation, peaked at 3 weeks in both BMP-2 and BP-treated groups. OPN expression, a representative marker of the late stage of osteogenic differentiation, reached its highest level at 4 weeks in both BMP-2 and BP-treated groups. Notably, the BMP-2-treated groups exhibited consistently high expression levels of RUNX2, ON, and OPN for the entire 4-week period. It is also worth noting that although the BP-treated group exhibited slightly lower expression levels

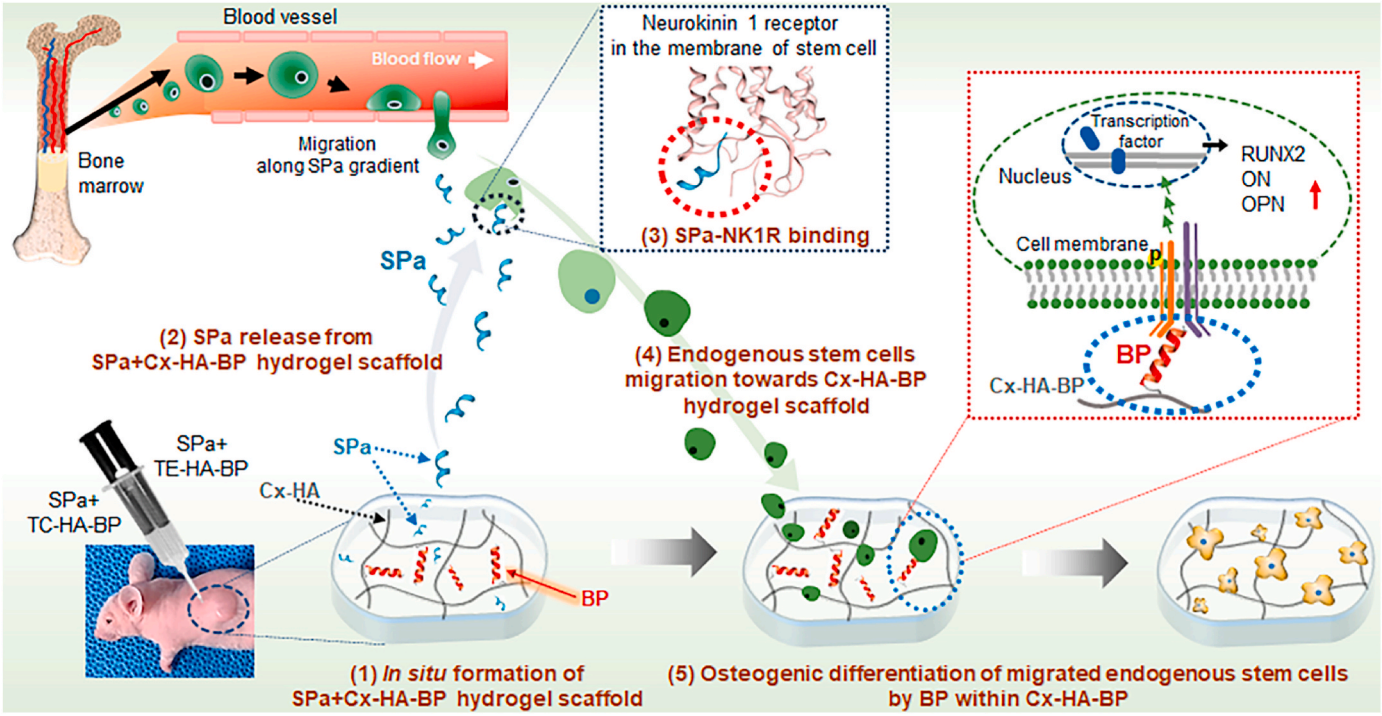

Fig. 1. Schematic illustration of (1) *in situ* hydrogel scaffold formation of SPa + Cx-HA-BP, (2) SPa release from SPa + Cx-HA-BP scaffold, (3) SPa binding to NK1R on endogenous stem cells, (4) migration of endogenous stem cells towards the Cx-HA-BP hydrogel scaffold, and (5) osteogenic differentiation of the migrated endogenous stem cells within Cx-HA-BP scaffold (The image was created by H.E.K. and M.S.K. using Adobe Photoshop 24.0.1 software).

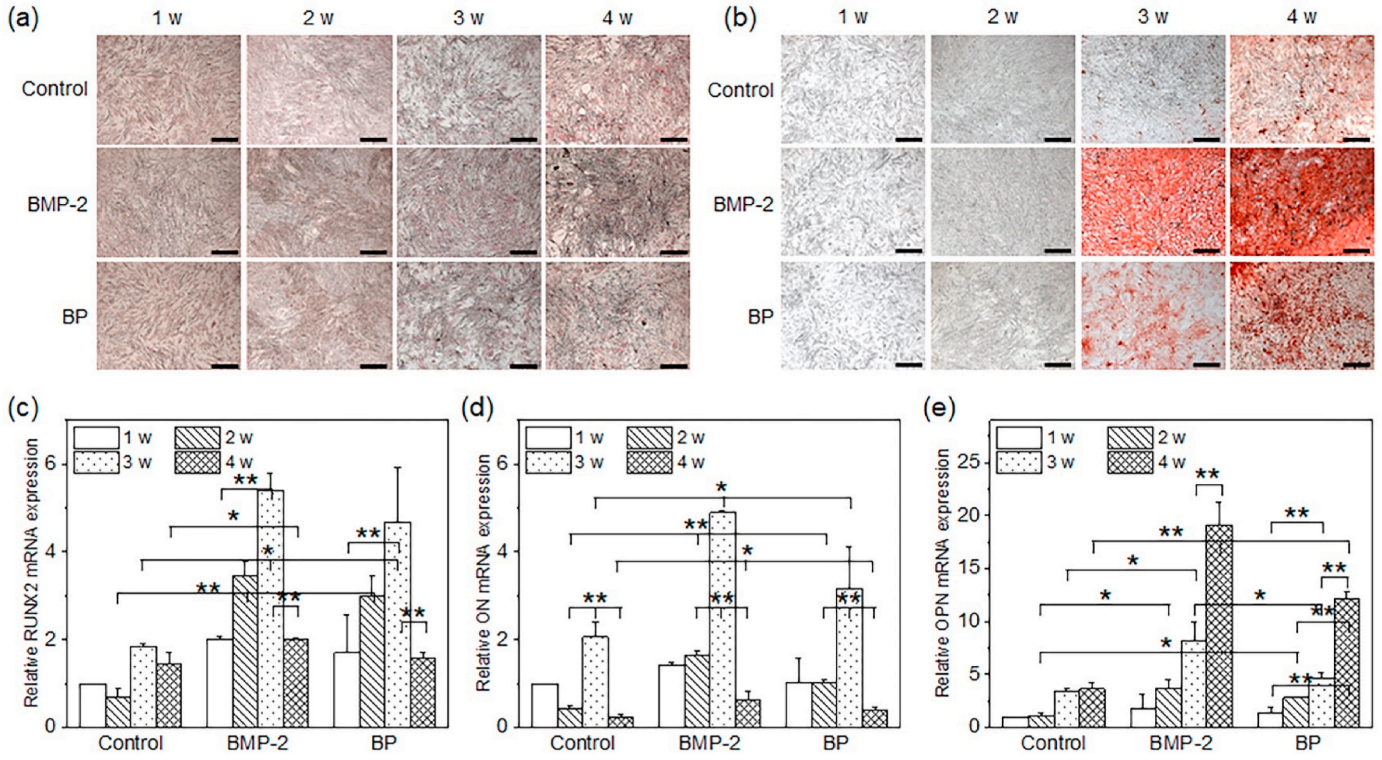

Fig. 2. *In vitro* osteogenic differentiation of hMSCs by BMP-2 or BP. (a) Von Kossa and (b) Alizarin red S staining for the *in vitro* osteogenic differentiation of hMSCs in osteogenic medium (control) and osteogenic medium containing BMP-2 or BP (magnification: 50×; scale bars: 500 μm) and gene expression of (c) RUNX2, (d) ON, and (e) OPN after weeks 1, 2, 3, and 4 through the *in vitro* osteogenic differentiation of hMSCs in osteogenic medium (control) and osteogenic medium containing BMP-2 or BP (*$p < 0.05$, **$p < 0.001$). (For interpretation of the references to color in this figure legend, the reader is referred to the Web version of this article.)

compared to the BMP-2-treated group, its expression levels were still higher than those of the control group. Taken together, these results confirm that BP derived from the BPM-2 sequence can effectively induce osteogenic differentiation in hMSCs.

3.2. Preparation and characterization of injectable scaffolds

To induce the osteogenic differentiation of endogenous stem cells migrating towards Cx-HA, Cx-HA-BP was produced by separately incorporating BP into TE-HA and TC-HA using a chemical method. First, TE and TC were individually combined with HA to produce TE-HA and TC-HA. ^{1}H NMR spectral analyses confirmed the presence of the characteristic peaks of TE or TC and BP in the obtained TE-HA and TC-HA, and the TE-HA-BP and TC-HA-BP (Figs. S1 and S2). The degrees of TE and TC substitution on the carboxylic groups in HA were confirmed to be above 90 % of the theoretical amount based on their C/N ratios in elemental analysis (Table S2). Next, BP was allowed to chemically react with TE-HA and TC-HA. Elemental analyses revealed that the degrees of BP substitution in the resulting TE-HA-BP and TC-HA-BP were respectively above 85 % and 92.5 % of the theoretical amount. Mixing TE-HA-BP and TC-HA-BP facilitated the rapid formation of Cx-HA-BP through click crosslinking. For comparison, equal amounts of BP as those chemically incorporated in the above-described conjugates were also physically incorporated into the hydrogels, resulting in the formation of Cx-HA+BP.

Next, the rheological properties of HA, Cx-HA, and Cx-HA-BP were analyzed to assess the viscosities of the prepared conjugates (Fig. 3a–c). The complex viscosity of Cx-HA and Cx-HA-BP was approximately 22–26 times higher than that of HA. The phase angles (tan δs) of Cx-HA and Cx-HA-BP, calculated from loss/storage modulus, were 0.18 and 0.12 (i.e., substantially less than 1), indicating that Cx-HA and Cx-HA-BP were significantly stiffer and more hydrogel-like than HA. Notably, Cx-HA-BP exhibited slightly higher complex viscosity and tan δ than Cx-HA, suggesting that the chemical incorporation of BP had a subtle effect on the hydrogel properties of the original Cx-HA.

To evaluate the injectability of hydrogels, [TE-HA and TC-HA] and [TE-HA-BP and TC-HA-BP] with and without SPa were loaded into a dual-barrel syringe (Fig. 3d). All formulations were ejected without clogging for over 20 s through a 26-G syringe needle. The formulations formed Cx-HA, Cx-HA-BP, SPa + Cx-HA, and SPa + Cx-HA-BP hydrogel scaffolds immediately in empty vials and even in vials filled with DW (Fig. S3), whereas HA alone readily dissolved in DW. This suggested that the click crosslinking between TE and TC in the formulations containing BP or SPa occurred rapidly, thereby promoting the formation of hydrogel scaffolds. Next, the structural characteristics of the formed HA, Cx-HA, and Cx-HA-BP hydrogel scaffolds were assessed via scanning electron microscopy (SEM) (Fig. S3). Cx-HA and Cx-HA-BP exhibited a predominantly porous interconnected three-dimensional polyhedral structure, whereas the HA hydrogel scaffold alone exhibited a tightly packed structure with small pores. The conjugates were then loaded into a dual-barrel syringe and the injection force exerted on each compartment of the syringe was measured by applying a constant force using an Instron universal testing machine (Fig. 3e and f). The injection force for HA alone was recorded at 4.4 N. For Cx-HA [TE-HA and TC-HA] and Cx-HA-BP [TE-HA-BP and TC-HA-BP], both with and without SPa, a slightly increased injection force of 6.7–7.1 N was observed. This suggests that formulations containing BP and/or SPa required a minor increase in injection force, although the difference was deemed negligible. This observation validates the suitability of all injection formulations as hydrogel scaffolds for subsequent experiments.

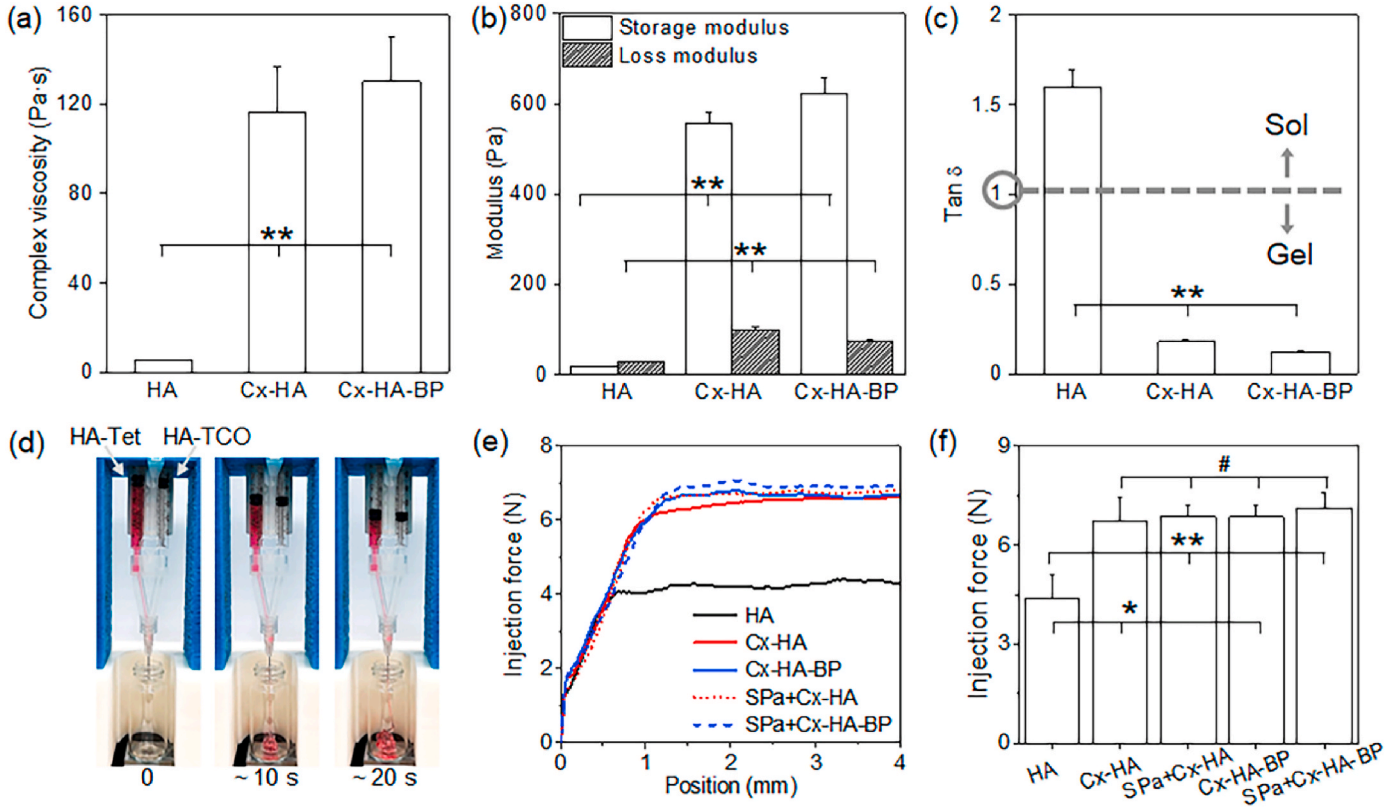

Fig. 3. Characterization of injectable formulation. (a–c) Rheological characterization of HA, Cx-HA and Cx-HA-BP and (d–f) injectability of injectable formulation ([HA alone], [TE-HA and TC-HA] [TE-HA-BP and TC-HA-BP] or [SPa + TE-HA and SPa + TC-HA]). (a) Complex viscosity, (b) storage and loss modulus, and (c) tan δ of HA, Cx-HA and Cx-HA-BP, (d) photo images of [TE-HA and TC-HA] charged in each compartment of a dual-barrel syringe with a 26-G syringe needle and injection into vial for 20 s (to form Cx-HA and Cx-HA-BP hydrogel scaffold), (e) injection force versus injection distance, and (f) maximum injection force of each formulation (*$p < 0.05$, **$p < 0.001$, $^{\#}p > 0.99$).

To confirm the *in vivo* formation and persistence of the hydrogel scaffold, hydrogel formulations containing a NIR probe, [HA-NIR alone] and [TE-HA-NIR and TC-HA-NIR], were subcutaneously injected into mice, after which scaffold formation was assessed via fluorescence imaging (Fig. S4). After subcutaneous injection, the formulations immediately emitted a pink NIR fluorescent signal. HA-NIR exhibited pink fluorescence at 1 day but not at 3 days, whereas the Cx-HA-NIR of the mice injected with [TE-HA-NIR and TC-HA-NIR] displayed immediate NIR-derived pink fluorescence, which persisted for more than 42 days. These findings suggest that the Cx-HA hydrogel scaffold remained within the injected tissue throughout the entirety of the animal experiment.

3.3. *In vitro* cytotoxicity and osteogenic differentiation of hMSCs

Although HA and peptides such as BP or SPa are generally considered safe and biocompatible materials, our study assessed the *in vitro* cytotoxicity of BP alone and SPa alone, as well as injectable formulations of Cx-HA, Cx-HA+BP, Cx-HA-BP, SPa + Cx-HA, and SPa + Cx-HA-BP using hMSCs (Fig. 4A). The viability of hMSCs in the bottom chamber was examined following incubation with BP alone or SPa alone and the injectable formulations, with BP alone or SPa alone in the upper chamber. A control experiment was also conducted without peptides or injectable formulations. Both BP alone or SPa alone and the injectable formulations were able to diffuse from the upper chamber to the bottom chamber, making contact with the hMSCs. Notably, hMSC viability did not vary significantly in response to different concentrations of BP alone or SPa alone, nor did it vary among the different injectable formulations ($^{\#}p > 0.99$). Furthermore, the hMSCs proliferated at a consistent rate over time with both BP alone or SPa alone and all injectable formulations, suggesting the absence of cytotoxic effects.

Subsequently, *in vitro* osteogenic differentiation was investigated by incubating hMSCs on the injectable formulations of Cx-HA, Cx-HA+BP, and Cx-HA-BP. Osteogenic differentiation was monitored by examining the expression of RUNX2, ON, and OPN mRNAs via RT-PCR (Fig. 4B). Interestingly, the expression of these genes was minimal in hMSCs incubated on Cx-HA even at week four. In contrast, the expression of RUNX2, ON, and OPN on Cx-HA+BP and Cx-HA-BP was significantly elevated. RUNX2 and ON, expressed in the early stage of osteogenic differentiation, were highly expressed in the presence of both Cx-HA+BP and Cx-HA-BP for 2 or 3 weeks and decreased by the 4th week. OPN expression, a marker of the late stage of osteogenic differentiation, gradually increased, reaching its peak at 4 weeks on both Cx-HA+BP and Cx-HA-BP. This trend in gene expression was consistent with earlier results (Fig. 2), indicating that BP induced the osteogenic differentiation of hMSCs. Moreover, the expression of RUNX2, ON, and OPN in hMSCs incubated on Cx-HA-BP was higher than in those cultivated on Cx-HA+BP. Specifically, the quantitative expression of these genes in the Cx-HA-BP group was approximately 2-fold higher than that of the Cx-HA+BP group at the time of maximal gene expression. This result suggests that BP, when physically mixed with Cx-HA and diffused into the media, could induce osteogenic differentiation at a relatively low level. In contrast, Cx-HA-BP, where BP was chemically bound to Cx-HA, resulted in a sustained and efficient induction of osteogenic differentiation. This suggests that BP, remains effective for an extended period when chemically bound to Cx-HA, continuously promoting the osteogenic differentiation of hMSCs. Collectively, these findings demonstrate that chemically loaded BP in Cx-HA efficiently induces the osteogenic differentiation of hMSCs.

3.4. *In vitro* migration assay of hMSCs toward SPa or SP and SP + Cx-HA or SPa + Cx-HA

To assess the migration-inducing effect of SPa on hMSCs, cell

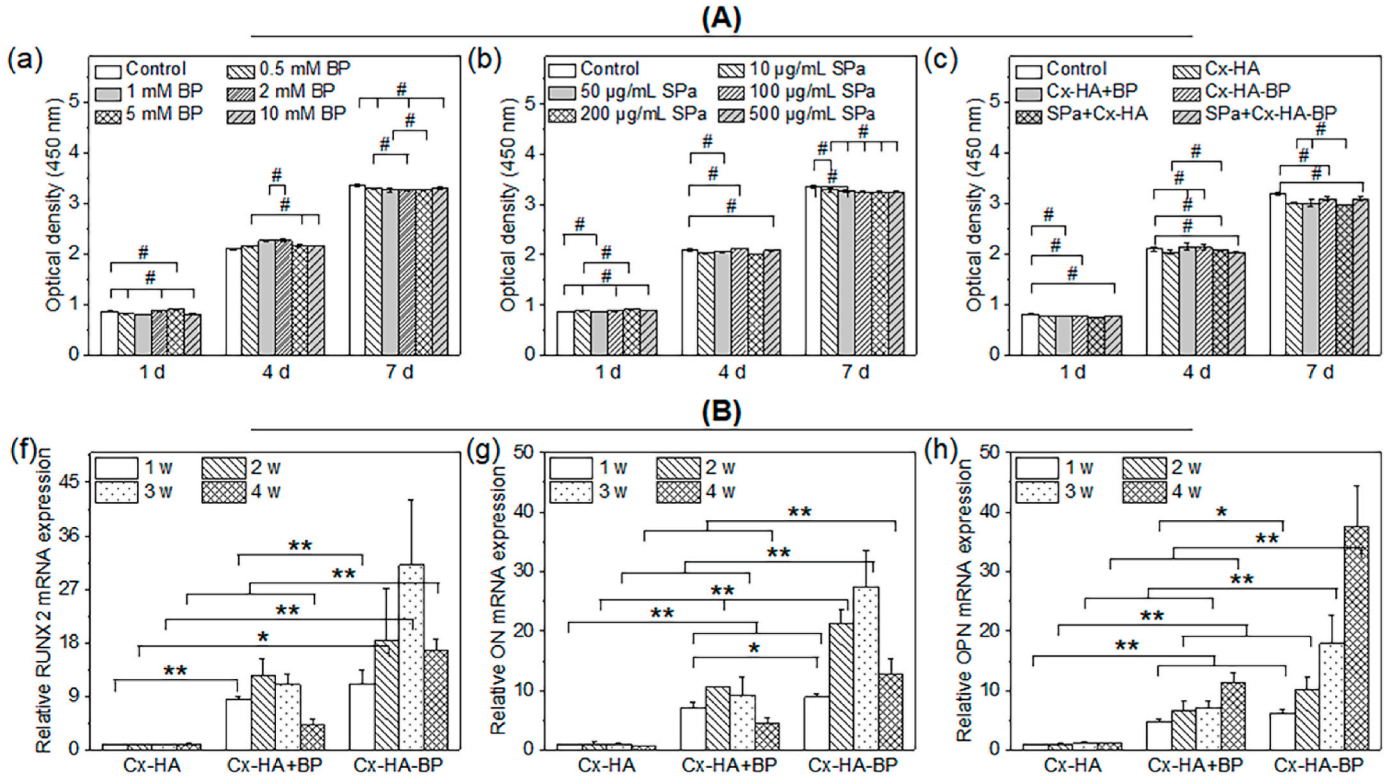

Fig. 4. *In vitro* evaluations of hMSC viability (A) and osteogenic differentiation (B). *In vitro* viability of hMSC (a) without (control) and with BP (0.5 mM, 1 mM, 2 mM, 5 mM, 10 mM), (b) without (control) and with SPa (10 μg/mL, 50 μg/mL, 100 μg/mL, 200 μg/mL, 500 μg/mL), and (c) without (control) and with Cx-HA, Cx-HA+BP, Cx-HA-BP, SPa + Cx-HA and SPa + Cx-HA-BP hydrogel scaffolds by CCK-8 assay ($^{\#}p > 0.95$). *In vitro* osteogenic differentiation of hMSCs in Cx-HA, Cx-HA+BP, and Cx-HA-BP hydrogel scaffolds, gene expression of (f) RUNX2, (g) ON, and (h) OPN after weeks 1, 2, 3, and 4 ($^{*}p < 0.05$, $^{**}p < 0.001$, $^{\#}p > 0.99$).

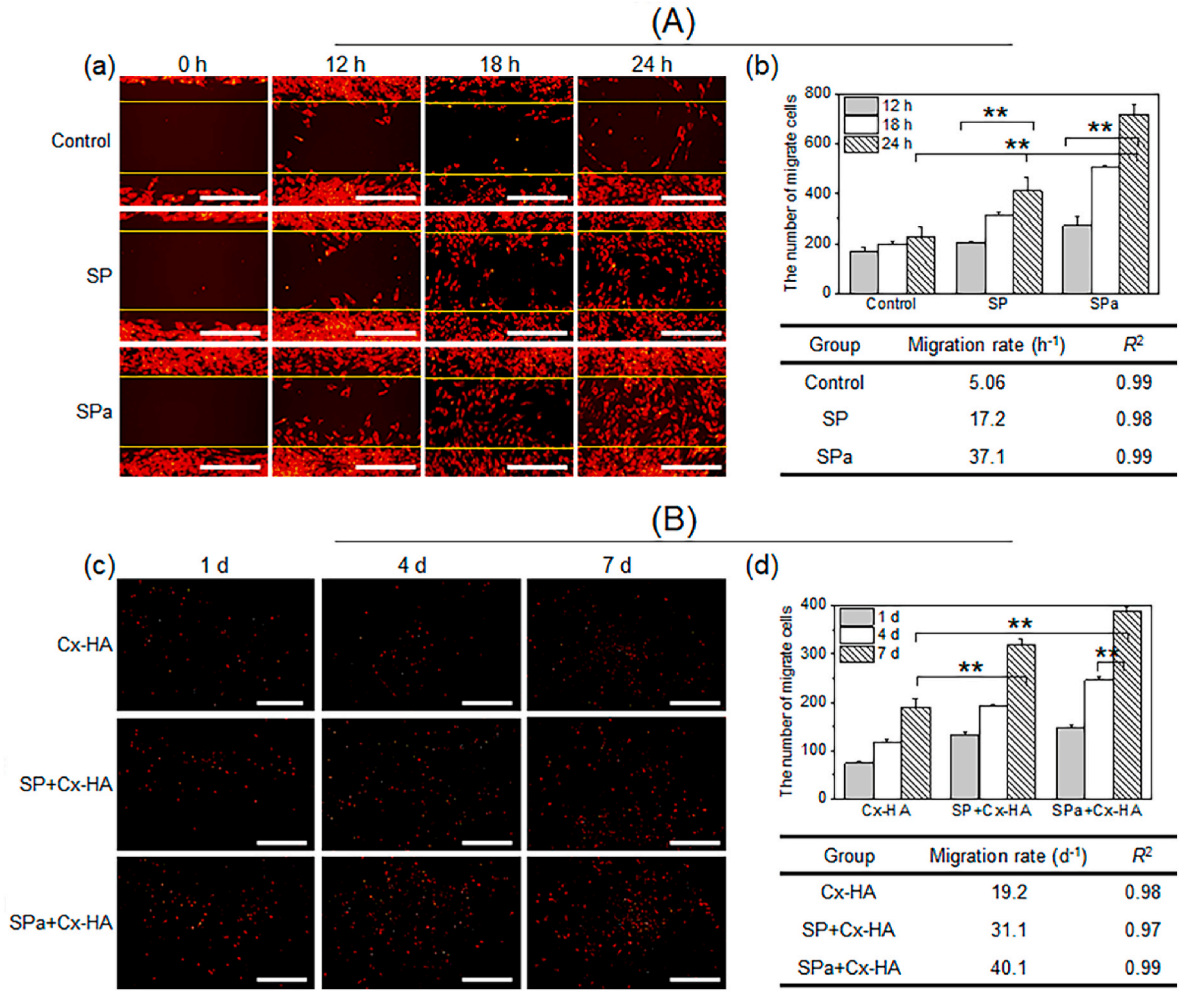

Group	Migration rate (h^{-1})	R^2
Control	5.06	0.99
SP	17.2	0.98
SPa	37.1	0.99

Group	Migration rate (d^{-1})	R^2
Cx-HA	19.2	0.98
SP+Cx-HA	31.1	0.97
SPa+Cx-HA	40.1	0.99

Fig. 5. *In vitro* migration assay by (A) wound field assay through (a) fluorescent images of PKH-hMSCs (magnification 100×; scale bars represent 500 μm) and (b) the counted number (**$p < 0.001$) and migration rate of migrated hMSCs in culture medium (control) or medium containing SP or SPa on 0 h, 12, 18, and 24 h, and (B) *in vitro* migration assay of PKH-hMSCs toward Cx-HA, SP + Cx-HA and SPa + Cx-HA hydrogel scaffolds by transwell plate through (c) fluorescent images of migrated PKH-hMSCs (magnification 40×; scale bars represent 1000 μm) and (d) the counted number (**$p < 0.001$) and migration rate.

migration was evaluated through a wound field assay to examine the effects of SP and SPa, as well as a transwell migration assay to explore the effects of SP or SPa released from SP + Cx-HA and SPa + Cx-HA (Fig. 5 and Figs. S5–7). Cell migration is a crucial process whereby cells alter their position in response to changes in the external environment to execute their functions. The wound field assay is commonly used to study the impact of chemoattractants such as SP and SPa in physiology (Fig. 5A). Initially, hMSC migration was assessed using the wound field assay. No migrated hMSCs were observed among monolayer-cultured hMSCs at 0 h. However, migrated hMSCs were observed after 12 h, and their number increased further with incubation time. The number of migrated hMSCs was plotted over incubation time, and the migration rate was calculated from the slope of the graph. The presence of SPa or SP accelerated the migration of hMSCs compared to conditions without chemoattractants. Furthermore, the migration rates of SP- and SPa-induced hMSCs were 17.2 and 37.1 cells/hour, respectively.

Subsequently, Cx-HA was mixed with SP or SPa, and the migration of hMSCs induced by Cx-HA, SP + Cx-HA, and SPa + Cx-HA was compared (Fig. 5B). PKH-hMSCs were loaded in the upper chamber, and Cx-HA, SP + Cx-HA, and SPa + Cx-HA were loaded in the bottom chambers. PKH-hMSCs in the upper chamber migrated toward the SP or SPa released from Cx-HA, and the number of migrated PKH-hMSCs was determined by counting the cells exhibiting red fluorescence. After one day, the number of PKH-hMSCs in the culture plate containing Cx-HA without SPa or SP increased gradually, albeit very slowly, possibly due to the migration of PKH-hMSCs toward the direction of gravity. In contrast, SP + Cx-HA and SPa + Cx-HA exhibited high migration of PKH-hMSCs, with a gradual increase over incubation time. The number of migrated PKH-hMSCs was plotted over incubation time, and the migration rates were calculated from the slope of the graph. The migration rates toward SP + Cx-HA and SPa + Cx-HA were 31.1 and 40.1 cells/day, respectively. Despite variations in the hMSC migration rates between the wound field assay and transwell migration assay, which were likely due to gravity, our findings confirmed that SPa was a more efficient chemoattractant than SP.

3.5. *In vivo* SP or SPa release profiles from HA or Cx-HA

To assess the *in vivo* SPa release from the hydrogel scaffolds, HA and [TE-HA and TC-HA] loaded with fluorescein-labeled SP-F or SPa-F were subcutaneously injected into animals. The release of SP-F or SPa-F from SPa-F + HA, SP-F + Cx-HA, and SPa-F + Cx-HA in the injected animals was assessed by monitoring the emitted green fluorescence (Fig. 6a). SPa-F + HA exhibited a clear fluorescent signal within 6 h but this signal was nearly undetectable by 1 day, which was likely due to the short *in vivo* residence time of HA (i.e., 2 days) (Fig. S8). In contrast, the green fluorescence intensity of SP-F + Cx-HA and SPa-F + Cx-HA also reached its maximum within 6 h of injection and showed a similar gradual

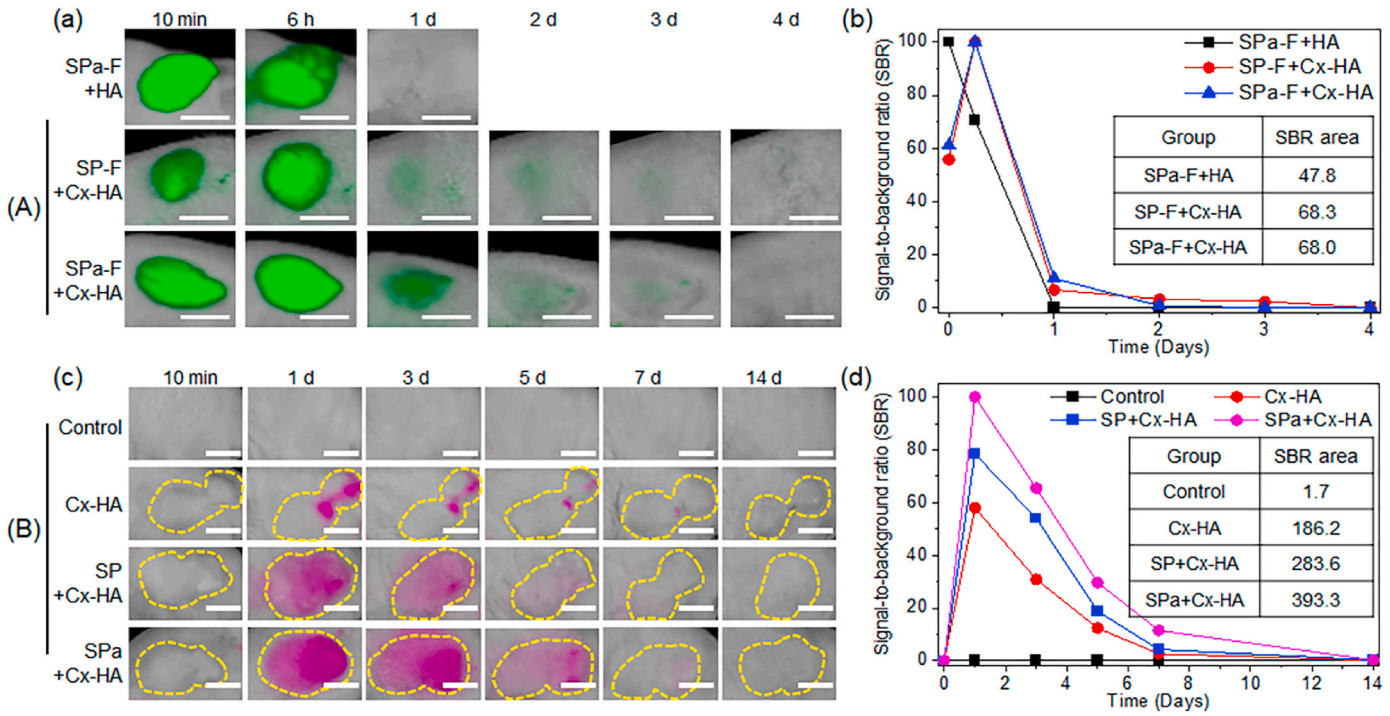

Fig. 6. *In vivo* release patterns of SP and SPa (A) and hMSCs migration (B). (a) *In vivo* real-time green images SP or SPa release profiles from HA or Cx-HA (scale bar = 1 cm) and (b) SBR ratios and area determined by *in vivo* green pink imaging obtained from each group at each time point. (c) *In vivo* real-time pink images of ICG-hMSCs migrated toward Cx-HA, SP + Cx-HA, and SPa + Cx-HA (scale bar = 5 mm) hydrogel *in vivo* and (d) SBR plot and area determined by *in vivo* NIR pink imaging obtained from each group at each time point. (For interpretation of the references to color in this figure legend, the reader is referred to the Web version of this article.)

decreasing pattern over time (Fig. 6b). However, despite exhibiting a relatively weak green fluorescent signal, SP-F + Cx-HA and SPa-F + Cx-HA maintained green fluorescence for 3 days, with little to no difference in green fluorescence intensity between SP-F and SPa-F from Cx-HA. Furthermore, when comparing the release of SPa-F from SPa-F + Cx-HA and SPa-F + Cx-HA-BP, there was little difference in SPa-F release between the two formulations. Collectively, our findings demonstrated that the release of SPa-F from Cx-HA or Cx-HA-BP was not significantly different.

3.6. *In vivo hMSC migration toward Cx-HA, SP + Cx-HA, and SPa + Cx-HA*

To investigate the migration of hMSCs induced by the hydrogel scaffold, injectable formulations (including Cx-HA, Cx-HA alone, SP + Cx-HA, and SPa + Cx-HA prepared with a dual-barrel syringe) were individually administered to animals. Next, ICG-hMSCs were injected into the tail of each animal with Cx-HA, SP + Cx-HA, and SPa + Cx-HA hydrogel scaffolds. The injected formulations formed a Cx-HA hydrogel scaffold, as indicated by the yellow dotted line in Fig. 6B, which was then monitored by observing changes in pink fluorescent signals (Fig. 6c). Animals that did not receive ICG-hMSCs (i.e., the controls) exhibited no pink fluorescence, confirming the absence of migration without the injection of ICG-hMSCs and SP or SPa. In the case of Cx-HA alone, pink fluorescence was observed on day 1 and a weak signal could still be detected at 7 days post-injection. This observation was likely attributed to the *in vivo* hMSC migration into Cx-HA alone relying on the interaction between HA and CD44. The carboxyl and hydroxyl groups of HA bind to the N-terminus of CD44 on hMSCs, acting as a docking site lined by a mixture of primarily basic and hydrophobic amino acids [22]. SP + Cx-HA and SPa + Cx-HA exhibited pink fluorescence throughout the entire area of the Cx-HA hydrogel scaffold on day 1. Pink fluorescence in SP + Cx-HA gradually decreased over time, being only barely detectable at 5 days and absent at 7 days. Conversely, SPa + Cx-HA displayed a more intense fluorescence signal on days 3 and 5 compared to SP + Cx-HA, with slight fluorescence still visible at 7 days. The SBR area of the fluorescence intensity for SPa + Cx-HA was 1.4 times greater than that of SP + Cx-HA and 2.1 times greater than that of Cx-HA alone (Fig. 6d). Collectively, these findings suggest that SPa facilitated the migration of ICG-hMSCs toward Cx-HA at a faster rate and in larger numbers compared to SP in the SP + Cx-HA formulation.

3.7. *In vivo BP maintenance of HA + BP-F, Cx-HA+BP-F, and Cx-HA-BP-F*

To evaluate the *in vivo* persistence of BP within the hydrogel scaffold, BF labeled with a green florescent marker (BP–F) was incorporated into the injectable formulations HA + BP-F, Cx-HA+BP-F, and Cx-HA-BP-F. These formulations were then subcutaneously injected into animals, after which the green fluorescence originating from BP-F was measured (Fig. 7). In the HA+BP-F group, the green fluorescence intensity observed at 10 min was maintained for 6 h, then rapidly decreased at 1 day, and almost disappeared thereafter. Cx-HA+BP-F exhibited a consistent fluorescence intensity until 6 h but fluorescence could still be detected at 7 days despite gradually attenuating. Notably, the fluorescence intensity of Cx-HA-BP-F was sustained for more than 28 days. This confirms that BP-F could be retained in Cx-HA for a longer period when BP was chemically bound to Cx-HA compared to being physically loaded into Cx-HA.

3.8. *In vivo osteogenic differentiation from endogenous stem cell migration*

To examine the *in vivo* osteogenic differentiation of endogenous stem cells after migration (i.e., without the direct injection of hMSCs), injectable formulations (including Cx-HA, SPa + Cx-HA, SPa + Cx-HA+BP, and SPa + Cx-HA-BP, prepared with a dual-barrel syringe) were injected into experimental animals, rapidly forming the corresponding

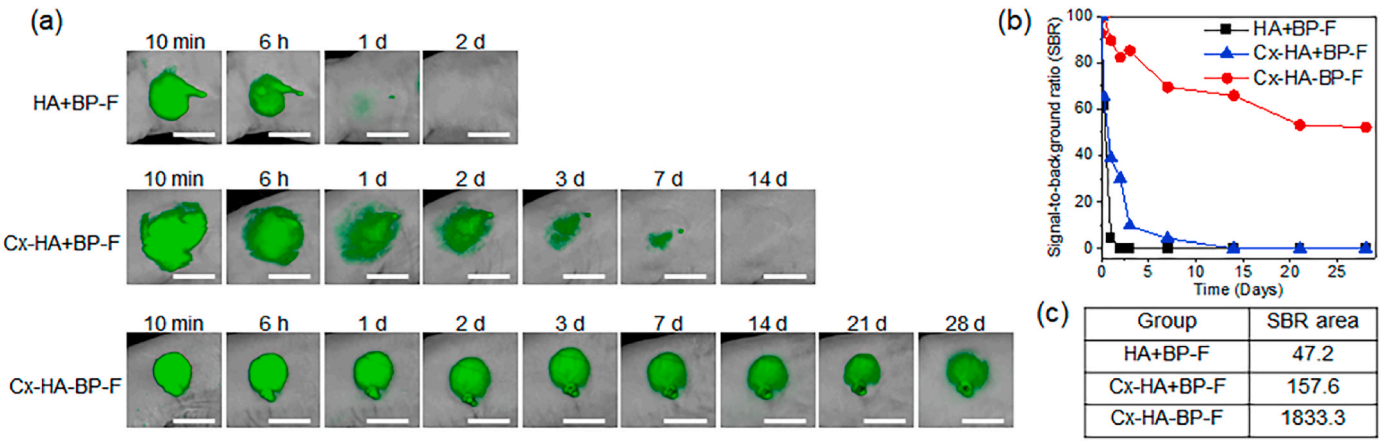

Group	SBR area
HA+BP-F	47.2
Cx-HA+BP-F	157.6
Cx-HA-BP-F	1833.3

Fig. 7. *In vivo* real-time images of the remained green fluorescent of BP-F from subcutaneous injected (a) HA+BP-F, (b) Cx-HA+BP-F and (c) Cx-HA-BP-F hydrogel scaffold (scale bar = 1 cm) for 28 days, (b) signal-to-background ratio (SBR) plot and (c) SBR area determined by *in vivo* NIR green imaging obtained from each group at each time point. (For interpretation of the references to color in this figure legend, the reader is referred to the Web version of this article.)

hydrogel scaffold in the injected tissue. To assess the osteogenic differentiation of endogenous stem cells that migrated in response to the SPa released from SPa + Cx-HA, SPa + Cx-HA+BP, and SPa + Cx-HA-BP, each hydrogel scaffold was surgically removed after 2, 4, and 6 weeks. All groups exhibited similar hydrogel sizes and shapes regardless of the implantation time, highlighting the *in vivo* persistence of the hydrogel scaffolds for 6 weeks. Von Kossa and Alizarin Red S staining were performed in all experimental groups, and the degree of *in situ* osteogenic differentiation was quantitatively determined based on the values of Von Kossa and Alizarin Red S-positive staining for each group using specialized imaging software (Fig. 8). Cx-HA alone without SPa and SPa + Cx-HA without BP exhibited little to no Von Kossa and Alizarin Red S-positive staining across all experimental periods. Among the SPa + Cx-HA+BP and SPa + Cx-HA-BP groups, low Von Kossa and Alizarin Red S-

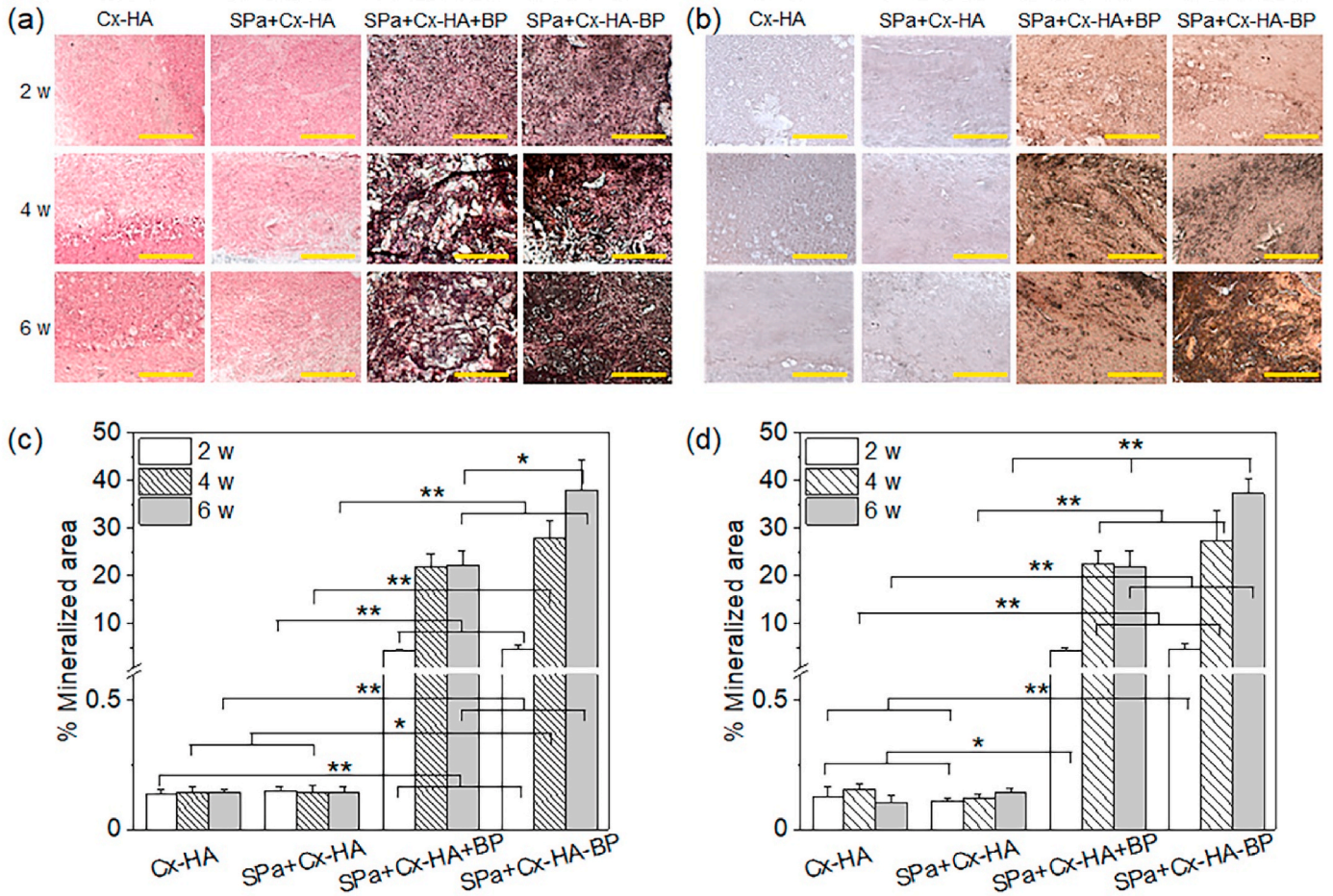

Fig. 8. *In vivo* osteogenic differentiation. (a,b) Staining and (c,d) the calculated mineralized areas of (a,c) Von kossa and (b,d) Alizarin red S during the *in vivo* osteogenic differentiation in Cx-HA, SPa + Cx-HA, SPa + Cx-HA+BP and SPa + Cx-HA-BP hydrogel scaffolds [(a and b) magnification: 50×; scale bars: 500 μm] (*$p < 0.001$, **$p < 0.005$). (For interpretation of the references to color in this figure legend, the reader is referred to the Web version of this article.)

positive staining were observed on week 2 but increased as the implantation time progressed. This result suggests that SPa likely induced the migration of endogenous stem cells toward the Cx-HA scaffold, after which the BP in the chemically bonded Cx-HA hydrogel scaffold induced the *in situ* osteogenic differentiation of the migrated endogenous stem cells. Additionally, the osteogenic differentiation of SPa + Cx-HA-BP was 1.5–1.7 times greater than that of SPa + Cx-HA+BP. This was likely because the chemically bonded BP was more stably maintained inside the hydrogel, making it more effective at inducing the osteogenic differentiation of endogenous stem cells that migrated toward the Cx-HA scaffold in response to SPa.

3.9. *In vivo* gene expression of hMSCs migrated toward hydrogels

Next, mRNA was extracted from the scaffolds of all examined groups. The expression levels of the RUNX2, ON, and OPN genes were quantified via real-time PCR to assess the effects of the hydrogel formulations on osteogenic differentiation (Fig. 9). Cx-HA alone induced little expression of RUNX2, ON, and OPN at 2, 4, and 6 weeks. In contrast, RUNX2, ON, and OPN were highly expressed in the SPa + Cx-HA+BP and SPa + Cx-HA-BP groups at 2, 4, and 6 weeks. These expression patterns were consistent with the *in vitro* results. RUNX2 and ON expression was low at 2 weeks, reached its highest point in the intermediate stage at 4 weeks, and decreased at 6 weeks. RUNX2 and ON expression in SPa + Cx-HA-BP was 3–5 times higher at 4 weeks and 4–9 times higher at 6 weeks than that of SPa + Cx-HA+BP. OPN expression, a marker for the late stage of osteogenesis, gradually increased in SPa + Cx-HA-BP and was highest at 6 weeks. OPN expression in the SPa + Cx-HA-BP group was 7 times higher than that of the SPa + Cx-HA+BP group at 6 weeks. The BP in the chemically bonded Cx-HA hydrogel scaffold induced higher expression of RUNX2, ON, and OPN compared to the physically loaded BP in Cx-HA. These findings demonstrated that chemically bonded BP induced high *in situ* osteogenic differentiation of the endogenous stem cells migrated by SPa released from Cx-HA. Collectively, our findings confirm that, upon SPa-induced migration, the endogenous stem cells underwent *in situ* osteogenic differentiation due to the presence of BP within the Cx-HA-BP scaffold. Taken together, our findings indicate that chemically loaded BP in Cx-HA steadily induced osteogenic differentiation of endogenous stem cells for a prolonged period.

4. Discussion

The inherent limitations in the self-healing capabilities of mammalian tissues have sparked a shift in regenerative medicine towards utilizing the body's own mechanisms for tissue repair. This approach, which eliminates the need for external cell sources, shows great promise for clinical use. Therefore, utilizing endogenous stem cells capable of self-renewal and differentiation into specific cell types both *in situ* and *in vivo* has garnered increasing attention due to their promising applicability in tissue regeneration therapies [23–25]. Our study sought to develop a novel strategy to enhance the migration of endogenous stem cells toward scaffolds, thereby promoting bone tissue formation. However, several factors must be considered to effectively implement this strategy, including identifying chemicals that attract the stem cells, selecting suitable hydrogel scaffolds to guide their movement, and assessing the osteogenic differentiation potential of endogenous stem cells.

HA is widely considered a uniquely well-suited biomaterial for these purposes due to its non-immunogenic nature and the presence of multiple functional chemical groups in its structure [26–30]. The introduction of click cross-linking sites and BP into HA, coupled with the physical addition of SPa, resulted in an injectable SPa + Cx-HA-BP hydrogel scaffold. This scaffold, which stimulates endogenous stem cell migration through the release of SPa, demonstrated no cytotoxicity. Additionally, the Cx-HA hydrogel alone demonstrated the ability to capture hMSCs, facilitated by its binding to the CD44 receptor on the surface of stem cells. These observations highlight its role in attracting these cells to the scaffold [22].

While traditional BMP is effective for bone regeneration, BP offers the advantages of cost-effectiveness and stability [20,29,30]. Our study confirmed the osteogenic differentiation potential of hMSCs induced by BP, rivaling the efficiency of BMP2 [31,32]. To ensure the sustained availability of BP within the scaffold, we explored both physical and chemical loading methods. Chemically incorporating BP into Cx-HA-BP resulted in prolonged retention, extending its availability and enhancing efficient osteogenic differentiation.

Effective chemoattractants play a crucial role in optimizing endogenous stem cell-based tissue regeneration. Our findings confirmed that ICG-labeled hMSCs injected into the tail vein migrated through blood vessels to other organs and ultimately migrated toward hydrogels loaded with SPa or SP. Among these, SPa emerged as a potent inducer of stem cell migration [9]. The SPa-loaded Cx-HA hydrogel successfully recruited migrating hMSCs, facilitating dynamic interaction between the scaffold and endogenous stem cells. Additionally, our study revealed that SPa outperformed SP in recruiting hMSCs, underscoring the importance of selecting appropriate chemoattractants.

However, when ICG is injected intravenously, self-quenching occurs due to binding to proteins and other biomolecules, leading to reduced fluorescence efficacy. Consequently, ICG has an initial half-life of 3–4 min when injected intravenously [33]. In our study, we observed that the fluorescence signal of ICG-labeled hMSCs migrating to the hydrogel after tail vein injection gradually decreased and disappeared after 3–5 days.

Endogenous stem cells can migrate from surrounding tissue niches

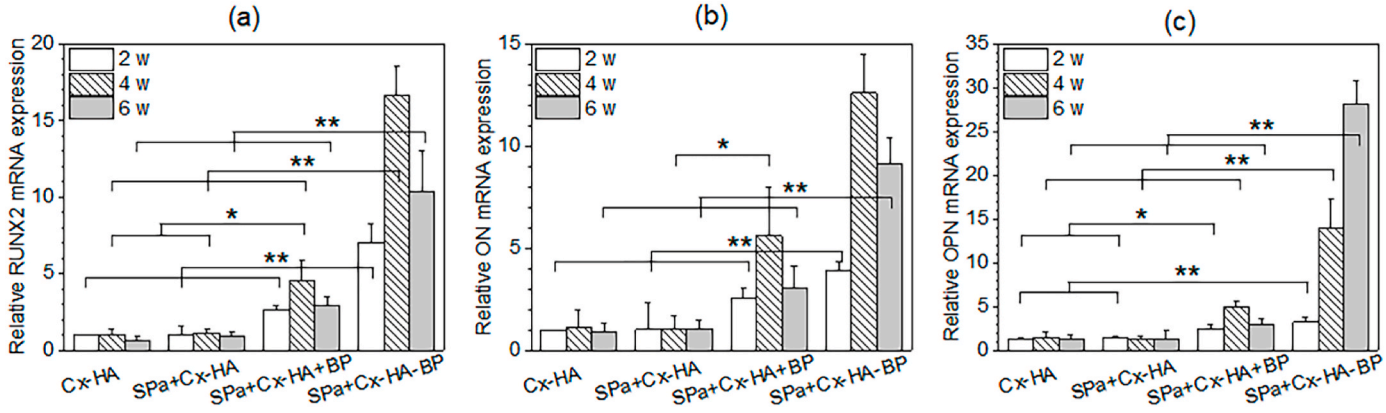

Fig. 9. *In vivo* osteogenic differentiation. Gene expression of (a) RUNX2, (b) ON and (c) OPN during the *in vivo* osteogenic differentiation in Cx-HA, SPa + Cx-HA, SPa + Cx-HA+BP and SPa + Cx-HA-BP hydrogel scaffold (*$p < 0.001$, **$p < 0.005$).

through interstitial migration induced by SPa and SP without involving the vascular system. Therefore, we evaluated whether endogenous stem cells that migrated from their original tissue niches towards Cx-HA in response to SPa underwent BP-mediated osteogenic differentiation. Little to no osteogenic differentiation was observed on the Cx-HA hydrogel scaffold alone. Similarly, the SPa + Cx-HA hydrogel scaffold exhibited minimal osteogenic differentiation. In the tail vein injection experiment, we observed that the SPa + Cx-HA hydrogel scaffold effectively captured hMSCs. Therefore, the minimal osteogenic differentiation observed in the SPa + Cx-HA hydrogel scaffold suggested that osteogenic differentiation did not occur in the absence of BP. In contrast, when combined with SPa, both Cx-HA+BP and Cx-HA-BP hydrogel scaffolds exhibited prominent osteogenic differentiation staining. Although Cx-HA-BP demonstrated slightly stronger results compared to Cx-HA+BP, the difference was not substantial. These findings suggest that the migration of endogenous stem cells from tissue niches, likely induced by SPa in the Cx-HA-BP hydrogel, subsequently led to osteogenic differentiation of the migrated endogenous stem cells.

Gene expression analysis further supported the robust osteogenic potential of both physically and chemically incorporated BP in Cx-HA+BP and Cx-HA-BP. Chemically incorporated BP, as observed in Cx-HA-BP, exhibited over 4–9 times higher expression levels of genes associated with osteogenic differentiation compared to physically mixed BP in Cx-HA+BP. These findings indicated that SPa efficiently guided endogenous stem cells from their original tissue niches towards the hydrogel scaffold, where chemically bound BP induced significant and sustained osteogenic differentiation.

5. Conclusion

In summary, the development of SPa + Cx-HA-BP represents a significant advancement in tissue regeneration, introducing a meticulously engineered scaffold that orchestrates a series of events to facilitate optimal endogenous stem cell-based tissue repair. Our research not only demonstrates the controlled release of SPa, effectively guiding endogenous stem cells towards the hydrogel scaffold but also underscores the crucial role of chemically incorporated BP in promoting robust osteogenic differentiation. Notably, the proposed approach enabled sustained and substantial osteogenic differentiation throughout an extended period. The lasting influence of BP, retained within the Cx-HA scaffold through chemical incorporation, suggests the potential for long-term tissue regeneration, a critical aspect of clinical translation.

The implications of this study extend beyond the laboratory, presenting a novel strategy with promising applications in regenerative medicine. By harnessing the inherent potential of endogenous stem cells, the SPa + Cx-HA-BP scaffold provides a promising platform for tissue regeneration through natural healing mechanisms. With its controlled release dynamics and chemical integration, the SPa + Cx-HA-BP scaffold not only contributes to our scientific understanding of tissue repair but also holds great promise for practical biomedical applications. Additionally, ongoing research aims to enhance the recruitment efficiency of endogenous stem cells by enabling sustained release of SP, thus prolonging its presence on the scaffold. Nevertheless, additional efforts are needed to optimize the recruitment of endogenous stem cells from tissue niches by precisely controlling the duration of SP sustained release from the scaffold, in addition to enhancing the differentiation efficiency of endogenous stem cells.

CRediT authorship contribution statement

Hee Eun Kim: Visualization, Investigation, Formal analysis, Data curation. **Hyeon Jin Ju:** Visualization, Investigation, Formal analysis. **Shina Kim:** Validation, Investigation, Formal analysis. **Young Hun Kim:** Validation, Formal analysis. **Soyeon Lee:** Validation, Formal analysis. **Sangdun Choi:** Validation, Software, Methodology. **Hyun C. Yoon:** Validation, Resources, Methodology. **Hak Soo Choi:** Writing – review & editing, Visualization, Validation, Project administration. **Moon Suk Kim:** Writing – review & editing, Writing – original draft, Resources, Funding acquisition, Conceptualization.

Declaration of competing interest

The authors declare the following financial interests/personal relationships which may be considered as potential competing interests: Moon Suk Kim reports financial support was provided by Ajou University. Moon Suk kim reports a relationship with Ajou University that includes: employment. If there are other authors, they declare that they have no known competing financial interests or personal relationships that could have appeared to influence the work reported in this paper.

Data availability

Data will be made available on request.

Acknowledgments

This study was supported by the National Research Foundation of Korea (NRF) grants, Creative Materials Discovery Program (2019M3D1A1078938) and Priority Research Centers Program (2019R1A6A1A11051471), and Ministry of SMEs and Startups (20144041). The corresponding author would like to extend gratitude to Ms. Yejin Kim and Yejin Lee for their collaboration in performing the additional measurement of NMR.

Appendix ASupplementary data

Supplementary data to this article can be found online at https://doi.org/10.1016/j.mtbio.2024.101070.

References

[1] A.K. Gaharwar, I. Singh, A. Khademhosseini, Engineered biomaterials for in situ tissue regeneration, Nat. Rev. Mater. 5 (2020) 686–705.
[2] J. Gong, G. Zhu, Y. Zhang, B. Chen, Y. Liu, H. Li, Z. He, J. Zou, Y. Qian, S. Zhu, X. Hu, S. Rao, J. Cao, H. Xie, Z. Wang, W. Du, Aptamer-functionalized hydrogels promote bone healing by selectively recruiting endogenous bone marrow mesenchymal stem cells, Mater. Today Bio 23 (2023) 100854.
[3] A.K. Gaharwar, I. Singh, A. Khademhosseini, Engineered biomaterials for in situ tissue regeneration, Nat. Rev. Mater. 5 (2020) 686–705.
[4] W. Jiang, X. Xiang, M. Song, J. Shen, Z. Shi, W. Huang, H. Liu, An all-silk-derived bilayer hydrogel for osteochondral tissue engineering, Mater. Today Bio 17 (2022) 100485.
[5] A. De Pieri, Y. Rochev, D.I. Zeugolis, Scaffold-free cell-based tissue engineering therapies: advances, shortfalls and forecast, NPJ Regen. Med. 6 (2021) 18.
[6] H.S. Hong, J. Lee, E.A. Lee, Y.S. Kwon, E. Lee, W. Ahn, M.H. Jiang, J.C. Kim, Y. Son, A new role of substance P as an injury-inducible messenger for mobilization of CD29+ stromal-like cells, Nat. Med. 15 (2009) 425–435.
[7] Z. Yang, H. Li, Z. Yuan, L. Fu, S. Jiang, C. Gao, F. Wang, K. Zha, G. Tian, Z. Sun, B. Huang, F. Wei, F. Cao, X. Sui, J. Peng, S. Lu, W. Guo, S. Liu, Q. Guo, Endogenous cell recruitment strategy for articular cartilage regeneration, Acta Biomater. 114 (2020) 31–52.
[8] S.J. Kim, J.E. Kim, G. Choe, D.H. Song, S.J. Kim, T.H. Kim, J. Yoo, S.H. Kim, Y. Jung, Self-assembled peptide-substance p hydrogels alleviate inflammation and ameliorate the cartilage regeneration in knee osteoarthritis, Biomater. Res. 27 (2023) 40.
[9] S.H. Park, H.J. Ju, Y.B. Ji, M. Shah, B.H. Min, H.S. Choi, S. Choi, M.S. Kim, Endogenous stem cell-based in-situ tissue regeneration using electrostatically interactive hydrogel with a newly discovered substance p analog and VEGF-mimicking peptide, Small 17 (2021) 2103244.
[10] C.E. Gillman, A.C. Jayasuriya, Fda-approved bone grafts and bone graft substitute devices in bone regeneration, Mater. Sci. Eng., C 130 (2021) 112466.
[11] A. Saito, Y. Suzuki, S.I. Ogata, C. Ohtsuki, M. Tanihara, Activation of osteo-progenitor cells by a novel synthetic peptide derived from the bone morphogenetic protein-2 knuckle epitope, Biochim. Biophys. Acta 1651 (2003) 60–67.
[12] S.H. Park, J.Y. Park, Y.B. Ji, H.J. Ju, B.H. Min, M.S. Kim, An injectable click-crosslinked hyaluronic acid hydrogel modified with a bmp-2 mimetic peptide as a bone tissue engineering scaffold, Acta Biomater. 117 (2020) 108–120.
[13] D.Y. Kim, D.Y. Kwon, J.S. Kwon, J.H. Kim, B.H. Min, M.S. Kim, Stimuli-responsive injectable in situ-forming hydrogels for regenerative medicines, Polymer Rev 55 (2015) 407–452.

[14] J.I. Kim, D.Y. Kim, D.Y. Kwon, H.J. Kang, J.H. Kim, B.H. Min, M.S. Kim, An injectable biodegradable temperature-responsive gel with an adjustable persistence window, Biomaterials 33 (2012) 2823–2834.
[15] J.S. Kwon, S.M. Yoon, S.W. Shim, J.H. Park, K.J. Min, H.J. Oh, J.H. Kim, Y.J. Kim, Y.J. Jin, B.H. Choi, M.S. Kim, Injectable extracellular matrix hydrogel developed using porcine articular cartilage, Int. J. Pharm. 454 (2013) 183–191.
[16] S.H. Park, R.S. Kim, W.R. Stiles, M. Jo, L. Zeng, S. Rho, Y. Baek, J. Kim, M.S. Kim, H. Kang, H.S. Choi, Injectable thermosensitive hydrogels for a sustained release of iron nanochelators, Adv. Sci. 9 (2022) e2200872.
[17] Z. Zheng, Y. Tan, Y. Li, Y. Liu, G. Yi, C.Y. Yu, H. Wei, Biotherapeutic-loaded injectable hydrogels as a synergistic strategy to support myocardial repair after myocardial infarction, J. Contr. Release 335 (2021) 216–236.
[18] K. Choi, C.Y. Park, J.S. Choi, Y. Kim, S. Chung, S. Lee, C. Kim, S.J. Park, The effect of the mechanical properties of the 3D printed gelatin/hyaluronic acid scaffolds on hMSCs differentiation towards chondrogenesis, Tissue Eng. Reg. Med. 20 (2023) 593–605.
[19] G.R. Shin, H.E. Kim, H.J. Ju, J.H. Kim, S. Choi, H.S. Choi, M.S. Kim, Injectable click-crosslinked hydrogel containing resveratrol to improve the therapeutic effect in triple negative breast cancer, Mater. Today Bio 16 (2022) 100386.
[20] S. Lee, J. Seo, Y.H. Kim, H.J. Ju, S. Kim, Y.B. Ji, H.B. Lee, H.S. Kim, S. Choi, M. S. Kim, Enhanced intra-articular therapy for rheumatoid arthritis using click-crosslinked hyaluronic acid hydrogels loaded with toll-like receptor antagonizing peptides, Acta Biomater. 172 (2023) 188–205.
[21] J. Seo, S.H. Park, M.J. Kim, H.J. Ju, X.Y. Yin, B.H. Min, M.S. Kim, Injectable click-crosslinked hyaluronic acid depot to prolong therapeutic activity in articular joints affected by rheumatoid arthritis, ACS Appl. Mater. Interfaces 28 (2019) 24984–24998.
[22] D.S. Bhattacharya, D. Svechkarev, J.J. Souchek, T.K. Hill, M.A. Taylor, A. Natarajan, A.M. Mohs, Impact of structurally modifying hyaluronic acid on cd44 interaction, J. Mater. Chem. B 5 (2017) 8183–8192.
[23] T. Wang, Q. Huang, Z. Rao, F. Liu, X. Su, X. Zhai, J. Ma, Y. Liang, D. Quan, G. Liao, Y. Bai, S. Zhang, Injectable decellularized extracellular matrix hydrogel promotes salivary gland regeneration via endogenous stem cell recruitment and suppression of fibrogenesis, Acta Biomater. 169 (2023) 256–272.
[24] Y.K. Alshoubaki, B. Nayer, S. Das, M.M. Martino, Modulation of the activity of stem and progenitor cells by immune cells, Stem Cells Transl. Med. 11 (2022) 248–258.
[25] J.R. Soucy, L. Todd, E. Kriukov, M. Phay, V.V. Malechka, J.D. Rivera, T.A. Reh, P. Baranov, Controlling donor and newborn neuron migration and maturation in the eye through microenvironment engineering, Proc. Natl. Acad. Sci. U.S.A. 120 (2023) 37931105.
[26] Z. Liu, W. Lin, Y. Liu, Macrocyclic supramolecular assemblies based on hyaluronic acid and their biological applications, Acc. Chem. Res. 55 (2022) 3417–3429.
[27] H.J. Kim, K.K. Kim, I.K. Park, B.S. Choi, J.H. Kim, M.S. Kim, Hybrid scaffolds composed of hyaluronic acid and collagen for cartilage regeneration, Tissue Eng. Reg. Med. 9 (2012) 57–62.
[28] H. Ferreira, D. Amorim, A.C. Lima, R.P. Pirraco, A.R. Costa-Pinto, R. Almeida, A. Almeida, R.L. Reis, F. Pinto-Ribeiro, N.M. Neves, A biocompatible and injectable hydrogel to boost the efficacy of stem cells in neurodegenerative diseases treatment, Life Sci. 287 (2021) 120108.
[29] S.H. Park, J.S. Kwon, B.S. Lee, J.H. Park, B.K. Lee, J.H. Yun, B.Y. Lee, J.H. Kim, B. H. Min, T.H. Yoo, M.S. Kim, Bmp2-immobilized injectable hydrogel for osteogenic differentiation of human periodontal ligament stem cells, Sci. Rep. 7 (2023) 6603.
[30] S.H. Cho, K.K. Shin, S.Y. Kim, M.Y. Cho, D.B. Oh, Y.T. Lim, In situ-forming collagen/poly-γ-glutamic acid hydrogel system with mesenchymal stem cells and bone morphogenetic protein-2 for bone tissue regeneration in a mouse calvarial bone defect model, Tissue Eng. Reg. Med. 19 (2022) 1099–1111.
[31] Y. Oki, K. Kirita, S. Ohta, S. Ohba, I. Horiguchi, Y. Sakai, T. Ito, Switching of cell proliferation/differentiation in thiol-maleimide clickable microcapsules triggered by in situ conjugation of biomimetic peptides, Biomacromolecules 20 (2019) 2350–2359.
[32] I. Bilem, L. Plawinski, P. Chevallier, C. Ayela, E.D. Sone, G. Laroche, M.C. Durrieu, The spatial patterning of rgd and bmp-2 mimetic peptides at the subcellular scale modulates human mesenchymal stem cells osteogenesis, J. Biomed. Mater. Res. A. 106 (2017) 959–970.
[33] J. Meyer, A. Cunea, D. Sonntag-Bensch, P. Welker, K. Licha, F.G. Holz, S. Schmitz-Valckenberg, In vivo imaging of a new indocyanine green micelle formulation in an animal model of laser-induced choroidal neovascularization, IOVS (Investig. Ophthalmol. Vis. Sci.) 55 (2014) 6204–6212.